Opt Rev (2017) 24:27–32
DOI 10.1007/s10043-016-0291-x

REGULAR PAPER

Elimination of dispersion effect in a white-light scanning interferometer by using a spectral analyzer

Song-Jie Luo[1] · Osami Sasaki[1,2] · Yong-Xin Liu[1] · Xiao-Yan Li[1] · Zhi-Li Lin[1] · Ji-Xiong Pu[1]

Received: 24 July 2016 / Accepted: 5 November 2016 / Published online: 18 November 2016

Abstract A general equation of the interference signal of white-light scanning interferometer (WSI) and its Fourier transform are derived. Based on these equations, a new method for elimination of a dispersion effect in WSI is proposed to measure exactly a reflecting surface position. A dispersion phase caused by the two sides of unequal length in a beam splitter is detected with a spectrally resolved interferometer (SRI). A spectral distribution is obtained by using Fourier transform from an interference signal detected with a WSI. The spectral phase of the SRI is subtracted from the spectral phase of the WSI to get a dispersion-free spectral phase, which provides an improved complex-valued interference signal where a position of zero phase is almost equal to a position of maximum amplitude. An accurate measurement is achieved by using the position of zero phase.

✉ Song-Jie Luo
songjieluo@163.com

Osami Sasaki
osamija@gmail.com

Yong-Xin Liu
22254208@qq.com

Xiao-Yan Li
xiaoyanli@siom.ac.cn

Zhi-Li Lin
zllin2008@gmail.com

Ji-Xiong Pu
jixiong@hqu.edu.cn

[1] Fujian Provincial Key Laboratory of Light Propagation and Transformation, College of Information Science and Engineering, Huaqiao University, Xiamen 361021, Fujian, China

[2] Emeritus Prof., Niigata University, Niigata 950-2181, Japan

Keywords Interferometry · Optical time domain reflectometry · Phase measurement

1 Introduction

White-light scanning interferometer (WSI) has been used widely to measure three-dimensional shapes of reflecting surfaces and thin films. The interference signal produced by a reflecting surface of an object in a WSI has an envelop peak and a fringe peak along the scanning position of the reference surface. When there is no dispersion effect in the interference between the object and reference beams, the envelop peak and the fringe peak appear on the same scanning position in the interference signal. In this situation the interference signal is symmetrical with respect to the envelop and fringe peak where the optical path difference (OPD) is zero. Hence the position of the reflecting surface can be simply measured. In practical cases, however, the positions of the envelop peak and the fringe peak are not identical, so that various methods for determination of a reflecting surface position have been reported [1, 2]. These methods focus on the waveform of the interference signal itself, but it is very important to utilize a spectral distribution in wavenumber domain which is a Fourier transform of the interference signal [3, 4].

In Ref. [3] the spectral distribution of the detected interference signal was corrected to get a repaired interference signal whose full width at half maximum (FWHM) was much smaller compared to the detected signal. A dispersion phase detected in the WSI with a calibration sample was subtracted from the spectral phase detected in the WSI with a sample to be measured. The spectral amplitude distribution was also modified to a symmetric distribution such as Gaussian function. If the scanning

velocity of the reference surface is not constant, the detected dispersion phase contains an additional phase distribution caused by the non-constant scanning velocity. In Ref. [4] the position of a reflecting surface was determined by the gradient value of the liner component in the spectral phase distribution. This gradient value seems to be sensitive to noises contained in the interference signal as reported in Ref. [5].

The interference signal of WSI has been discussed under the assumption that the spectrum of the light source is Gaussian [1–6]. Hence it is not clear how the waveform of the interference signal is formed in general case such as non-Gaussian spectrum. On the other hand, it is easy to understand the spectral distribution of the interference signal of WSI in the situation that spectrally resolved interferometers (SRIs) have been applied to many fields. The spectral phase distribution can be obtained from the interference signal of an SRI by the signal processing using Fourier transform. This spectral phase distribution has been used for dispersion measurement [7, 8], and as another application it has been utilized to measure three-dimensional shape of a thin film [9].

The interference signal detected with a WSI is a real-valued function, and its complex-valued function is obtained by the signal processing using Fourier transform through its spectral distribution in wavenumber domain. Since the complex-valued interference signal (CVIS) of WSI is considered as being generated by adding CVISs of many different wavenumbers, the phase is zero and the amplitude is maximum at the position of the reflecting surface in the CVIS without the dispersion effect. When there is the dispersion effect, the position of zero phase and the position of maximum amplitude which are related strongly to the fringe peak and the envelop peak, respectively, are separated. The CVIS of WSI is similar as the reconstructed optical field generated by backpropagation of multiple-wavelength optical fields detected in a multiple-wavelength interferometer for measurement of a surface profile or a shape of thin film [5–10]. The position of the reflecting surface can be accurately determined by a position of zero phase nearest to the position of maximum amplitude in the CVIS containing noises, similarly as in the field reconstructed by the backpropagation.

In this paper, a general equation of the interference signal of WSI with a light source of an arbitrary spectrum and its Fourier transform are derived. But the configuration of WSI is simple as shown in Fig. 1, where the object and reference waves are collimated beams. Based on the derived equations, a new method for elimination of the dispersion effect in WSI is proposed and it is shown that the processing of the interference signal by Fourier transform in both scanning position domain and wavenumber domain is important to measure a reflecting surface position with a high measurement accuracy of the order of nm. First a spectral phase distribution is detected with an SRI which is simply implemented by using a spectrum analyzer in a WSI. This detected phase distribution is an exact dispersion phase existing in the WSI. It is shown that the dispersion phase is caused by the two sides of unequal length in a cubic beam splitter. Next position measurement is made with the WSI eliminating the dispersion effect. The spectral distribution in the wavenumber domain is obtained from the detected interference signal with Fourier transform. The spectral phase detected with the SRI is subtracted from the spectral phase detected with the WSI to get a dispersion-free spectral phase distribution. Inverse Fourier transform of the dispersion-free spectral distribution in the region of positive wavenumbers provides an improved CVIS where the position of zero phase is almost equal to the position of maximum amplitude. An accurate measurement is achieved by using the position of zero phase.

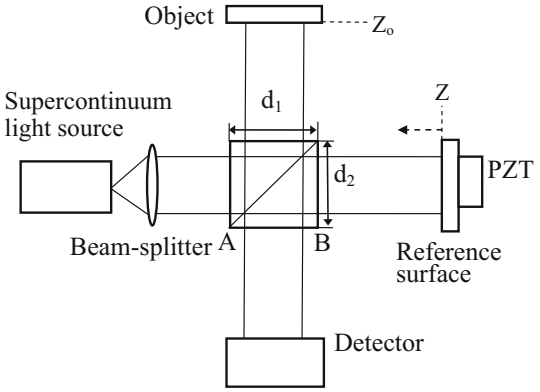

Fig. 1 Schematic of an interferometer using a supercontinuum light source

2 Theory

2.1 Signals in WSI

Figure 1 shows a Michelson interferometer which has a super continuum light source and a piezoelectric transducer (PZT). Position z of the reference surface is moved by the PZT. Denoting the position of object surface by z_o, the optical path difference (OPD) is $L = 2(z - z_o)$. When the PZT is moving and the detector is a photodiode in Fig. 1, the interferometer is a white-light scanning interferometer (WSI). The interference signal has the two components and one of them is constant during the scanning of z. Omitting this constant component, the interference signal is described as

$$S_v(z) = \int_{-\infty}^{\infty} I(\sigma)\cos[4\pi(z - z_o)\sigma + \varphi_v(\sigma)]d\sigma, \quad (1)$$

where σ is wavenumber, and $I(\sigma)$ is the spectral intensity of the light source. Phase $\varphi_v(\sigma)$ is an aberration phase. $I(\sigma)$ and $\varphi_v(\sigma)$ are defined in the region of $\sigma > 0$. Equation (1) is rewritten as

$$S_v(z) = \int_{-\infty}^{\infty} I(\sigma) e^{j\varphi_v(\sigma)} e^{j2\pi L\sigma} d\sigma + \int_{-\infty}^{\infty} I(\sigma) e^{-j\varphi_v(\sigma)} e^{-j2\pi L\sigma} d\sigma, \quad (2)$$

where $L = 2(z - z_o)$, and coefficient of 1/2 is omitted in the right side of Eq. (2) for simplicity. Expressing the inverse Fourier transform of $I(\sigma)e^{j\varphi_v(\sigma)}$ by $A(L)e^{j\alpha(L)}$, Eq. (2) can be reduced to a simple equation as follows:

$$S_v(z) = A(L)e^{j\alpha(L)} + A(L)e^{-j\alpha(L)} = 2A(L)\cos[\alpha(L)]. \quad (3)$$

Fourier transform is performed on $S_v(z)$ to get the CVIS of $S_v(z)$. By making terms of $e^{\pm j4\pi(z-z_0)\sigma}$ in Eq. (2) and regarding Eq. (2) as an inverse Fourier transform of $S_v(z)$, the Fourier transform of $S_v(z)$ in the region of positive wavenumbers is obtained from the first tem of Eq. (2) as

$$F_v(\sigma) = I(\sigma)e^{j\varphi_v(\sigma)}e^{-j4\pi z_o\sigma} \ (\sigma > 0). \quad (4)$$

The second term of Eq. (2) leads to the Fourier transform of $S_v(z)$ in the region of negative wavenumbers.

Therefore, from Eqs. (2) and (4) the CVIS of $S_v(z)$ is expressed by $A(2(z - z_o))\exp(j\alpha(2(z - z_o)))$ whose inverse Fourier transform is given by Eq. (4). This relation leads to the following characteristics: (1) when the aberration phase $\varphi_v(\sigma)$ is equal to zero, the amplitude of $A(2(z - z_o))$ is symmetric about the position z_o of the object surface which is equal to a position z_a of maximum amplitude of $A(L)$ and a position z_p of zero phase of $\alpha(L)$, (2) When $\varphi_v(\sigma)$ is not equal to zero, the position z_a and the position z_p are not identical and are not equal to the position z_o. Since the aberration phase $\varphi_v(\sigma)$ contains a dispersion phase, the dispersion phase is detected with a spectrally resolved interferometer to reduce the aberration phase close to zero value.

2.2 Dispersion phase in SRI

When the detector is a spectral analyzer and the PZT is stationary, the interferometer is a spectrally resolved interferometer (SRI) in Fig. 1. The interference signal has the two components and one of them is constant for a change of OPD. Omitting this constant component, the interference signal is expressed as

$$S_s(\sigma) = I(\sigma)\cos[2\pi L\sigma + \varphi_d(\sigma)], \quad (5)$$

where $\varphi_d(\sigma)$ is a dispersion phase. It is assumed that this dispersion phase is caused by a cubic beam splitter which has the two sides whose lengths are d_1 and d_2, respectively, and $d_\varepsilon = d_1 - d_2$ that is not equal to zero, as shown in Fig. 1. The two beams producing the interference signal pass through a point on the exit side of the beam splitter denoted by the line A-B in Fig. 1. The dispersion phase does not occur in the interference signal when the two beams propagate along the same path in a dispersive medium or the beam splitter. Hence the dispersion phase is generated after the incident single beam is split and until the split two beams are combined in the beam splitter. The length of the propagation path in the beam splitter along which the dispersion phase is generated is different along the line A-B. Therefore, by using a coefficient γ whose value changes linearly from 1 to 0 along the line A-B, the dispersion phase is given by

$$\varphi_d(\sigma) = 4\pi[n(\sigma) - 1]\gamma d_\varepsilon\sigma, \quad (6)$$

where $n(\sigma)$ is refractive index.

3 Experiments

In experiments, a supercontinuum light source was used and its spectral range was 500–1400 nm. Both the object and reference surfaces were wedged glass plates which could be regarded as having one reflecting surface. The reference surface was moved by the PZT at a constant velocity of 70 μm/s, and the sampling interval Δz of the interference signal was 7 nm in the WSI. The interference signal was detected with a photodiode at one point which corresponded to the midpoint of the line A-B. The data number N of the raw interference signal was 8192. Required data were selected from the raw data with a rectangular window as shown in Fig. 2. The other data outside the rectangular window were zero values. Fourier transform was performed on this interference signal of data number N. From properties of Fourier transform a linear component in phase of the Fourier transform of the interference signal will be decreased greatly when the peak position of the envelope of the interference signal is the origin of z axis. Hence a data at $z = 0$ in Fig. 2 was

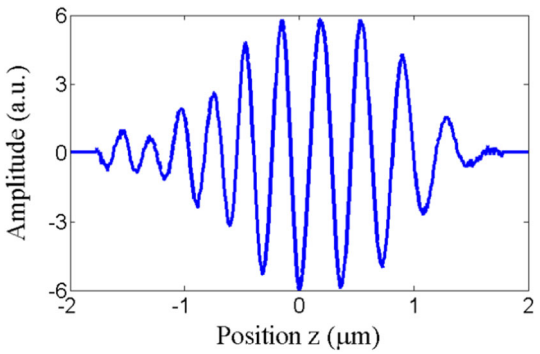

Fig. 2 Interference signal of the WSI

selected as the first data of the signal for the Fourier transform. The variable in the Fourier transform of the interference signal was wavenumber σ and its interval was $\Delta\sigma = 1/2\ N\Delta z = 8.8\times10^{-3}\ \mu m^{-1}$.

Figure 3 shows the Fourier transform of the interference signal given by Eq. (4), where Fig. 3a, b are the spectral amplitude and phase, respectively. The amplitude was almost zero outside the wavenumber range of 1.1–2.1 μm^{-1}. The rectangular window with the width of 1.1–2.1 μm^{-1} was multiplied by the Fourier transform of the interference signal. Inverse Fourier transform was performed on this windowed data to get the CVIS or $Ae^{j\alpha}$. Figure 4 shows the results of the inverse Fourier transform. The amplitude and phase distributions represent $A(2(z - z_0))$ and $\alpha(2(z - z_0))$, respectively, if the aberration phase $\varphi_v(\sigma)$is equal to zero. Then the position z_a of maximum amplitude and the position z_p of zero phase nearest to z_a are equal to z_o. However, in Fig. 4a the amplitude distribution has two peaks at the positions of −0.140 and 0.395 μm, respectively. If these positions are considered as the position z_a, the positions of z_p are −0.151 and 0.558 μm, respectively, as shown in Fig. 4b. Since it is difficult to decide a correct position of z_a from the two positions of z_a where the differences between the z_p and the z_a were 11 and 163 nm, respectively, an exact measurement could not be made.

In the SRI, the interference signal was detected with an optical spectral analyzer whose input face of the fiber was placed at the same point as in the WSI, and then $\gamma = 0.5$. The output of the spectrum analyzer was transformed from wavelength axis to wavenumber axis with an interpolation to get the interference signal with a constant interval of wavenumber which is equal to that in Fig. 3. Figure 5 shows the interference signal of the SRI in wavenumber domain, where the OPD was about 58 μm. Fourier transform was performed on the interference signal of Fig. 5, and the rectangular window with a width of $z = 26$–31 μm was multiplied by the Fourier transform of the interference signal. Inverse Fourier transform was performed on this windowed data to get the complex-valued interference signal of Fig. 5. Figure 6 shows its amplitude distribution which is almost the same as the amplitude of Fig. 3a. But these amplitude distributions do not contain large values around 1.3 μm^{-1} shown in Fig. 5. These strong and narrow spectral components produced a sinusoidal signal with a small amplitude which existed outside the rectangular windows used to get Figs. 3 and 6. These windows eliminated the sinusoidal signal, which resulted in the disappearance of the

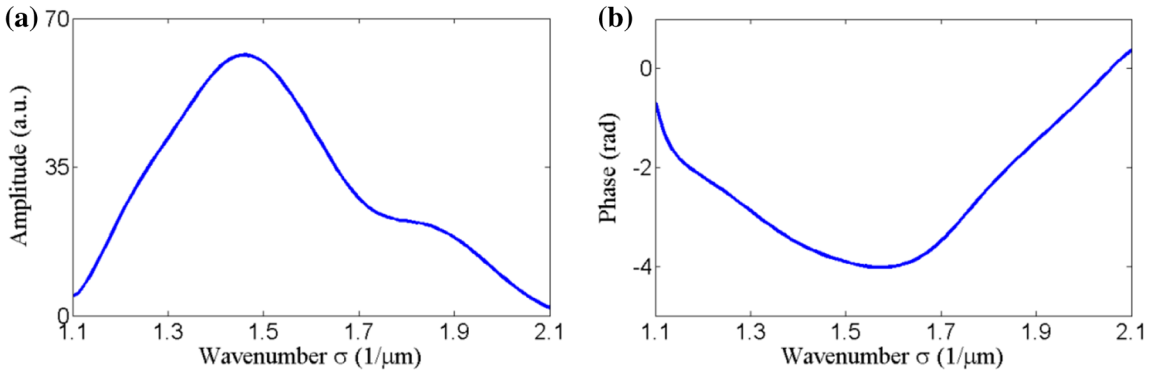

Fig. 3 Fourier transform of the interference signal of the WSI: **a** amplitude and **b** phase

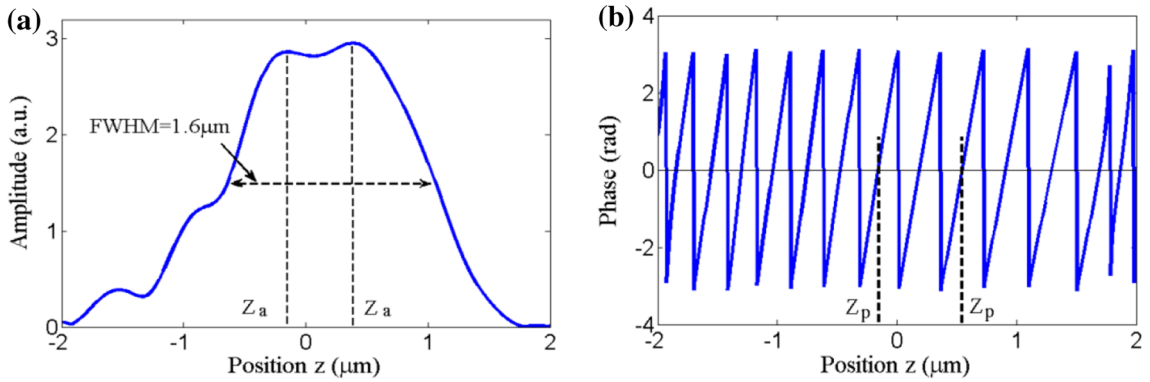

Fig. 4 Complex-valued interference signal of the WSI: **a** amplitude and **b** phase

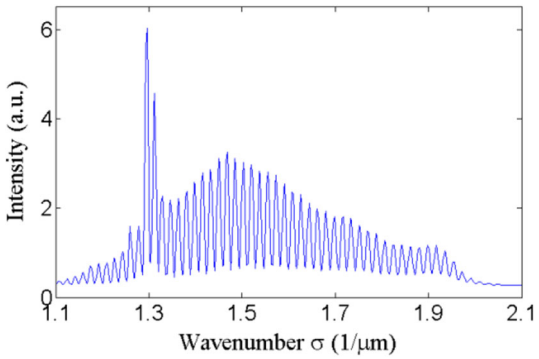

Fig. 5 Interference signal of the SRI

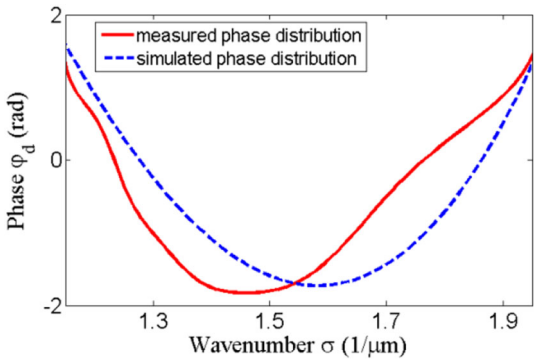

Fig. 7 Measured and simulated dispersion phase

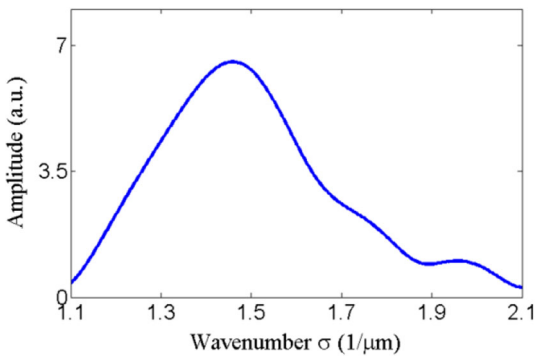

Fig. 6 Amplitude of the complex-valued interference signal of the SRI

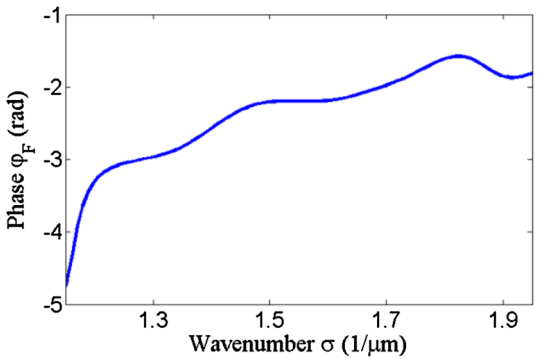

Fig. 8 Dispersion-free phase after subtracting the phase φ_d from the phase of Fig. 3b

large values around 1.3 μm^{-1}. Since the amplitude of the interference signal was almost zero outside the region from 1.15 to 1.95 μm^{-1} as shown in Fig. 6, the phase distribution of the complex-valued interference signal of Fig. 5 was used in this region. The linear and bias components were eliminated from the phase distribution to get the measured dispersion phase $\varphi_d(\sigma)$, as shown in Fig. 7. To examine if the measured dispersion phase satisfied Eq. (6) or not, values of Eq. (6) at $\gamma = 0.5$ were calculated by the Sellmeier equation of BK7 glass and changed the value of d_ε. When $d_\varepsilon = 90$-μm, the simulated dispersion phase was most similar with the one measured with the SRI, as shown in Fig. 7. It is estimated that the two phase distributions were not completely the same because there were other dispersive materials in the beam splitter such as adhesives and non-reflecting films. When the lengths of the two sides of the beam splitter were measured with a caliper gauge, the difference between the two sizes was about 100 μm. When the input face of the fiber of the optical spectral analyzer was moved along the line A-B, the magnitude of the dispersion phase changed almost linearly with the change of γ without a large change of its distribution.

By subtracting the dispersion phase φ_d measured with the SRI from the spectral phase of Fig. 3b measured with the WSI, the dispersion-free phase φ_f was obtained as shown in Fig. 8. The phase φ_f still had some non-linear component, which was regarded as being caused by a non-constant scanning velocity of the reference surface. The spectral phase of Fig. 3b was replaced by the phase φ_f of Fig. 8 and the amplitude of Fig. 3a was used to get the dispersion-free data in wavenumber domain. Inverse Fourier transform was performed on this data, and the results are shown in Fig. 9. The amplitude distribution approached to symmetrical one and its full width at half maximum (FWHM) decreased to 0.90 from 1.6 μm in Fig. 4a. The position z_a of maximum amplitude was −0.201 μm, and the position z_p of zero phase nearest to z_a was −0.203 μm, where the difference between the two positions was 2 nm. Other detected interference signals of the WSI also provided similar results where the FWHMs were about 0.9 μm and the differences between z_p and z_a were within several nanometers in the dispersion-free CVIS. The position z_o of the object could be exactly decided to be the value of z_p.

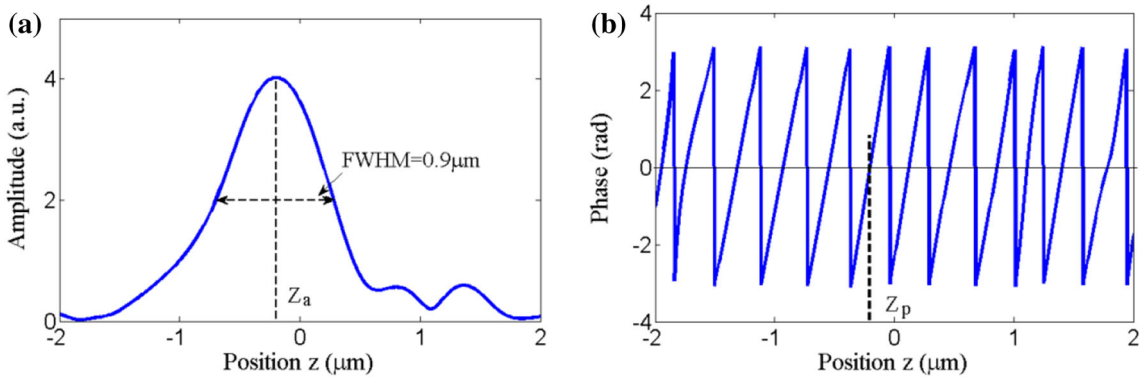

Fig. 9 Complex-valued interference signal of the WSI after elimination of the dispersion: **a** amplitude and **b** phase

4 Conclusion

It has been indicated from the experimental results of one reflecting surface and the expressions by Eqs. (3) and (4), how the existence of the aberration phase φ_v affects the amplitude and phase distributions of the CVIS. The dispersion phase φ_d was detected with the SRI. It has been made clear that the FWHM of the amplitude distribution and the difference between the z_p and the z_a could be greatly reduced in the CVIS by eliminating the dispersion phase φ_d from the aberration phase φ_v. The signal processing with Fourier transform between position and wavenumber domains was performed for the position measurement where the position z_p was considered as an exact position of the one reflecting surface.

In the near future it will be shown clearly by simulations and experiments of step shape measurements that the position of zero phase provides accurate position measurements. Also the phase distribution of the CVIS will be examined in detail.

Acknowledgements This research was supported by National Natural Science Foundation of China (NSFC) (61275203, 61505059 and 61575070), the Fujian Province Science Funds for Distinguished Young Scholar (No. 2015J06015) and the Natural Science Foundation of Fujian Province of China (No. 2014J05007).

References

1. Park, M.C., Kim, S.W.: Direct quadratic polynomial fitting for fringe peak detection of white light scanning interferograms. Opt Eng **39**(4), 952–959 (2000)
2. Pikálek, T., Fořt, T., Buchta, Z.: Detection techniques in low-coherence interferometry and their impact on overall measurement accuracy. Appl Opt **53**, 8463–8470 (2014)
3. de Groot. P.: Compensation of systematic effects in low coherence interferometry. Patent 7,522,288 (2009)
4. de Groot, P., Deck, L.: Surface profiling by analysis of white-light interferograms in the spatial frequency domain. J Mod Opt **42**, 389–401 (1995)
5. Sasaki, O., Tai, H., Suzuki, T.: Step-profile measurement by backpropagation of multiple-wavelength optical fields. Opt Lett **38**(18), 2683–2685 (2007)
6. Pavliček, P., Soubusta, J.: Measurement of the influence of dispersion on white-light interferometry. Appl Opt **43**, 766–770 (2004)
7. Pshenay-Severin, E., Setzpfandt, F., Helgert, C., Hübner, U., Menzel, C., Chipouline, A., Rockstuhl, C., Tünnermann, A., Lederer, F., Pertsch, T.: Experimental determination of the dispersion relation of light in metamaterials by white-light interferometry. J Opt Soc Am B **27**, 666–1254 (2010)
8. Luo, Z.Y., Zhang, S.N., Shen, W.D., Xia, C., Ma, Q., Liu, X., Zhang, Y.G.: Group delay dispersion measurement of a dispersive mirror by spectral interferometry: comparison of different signal processing algorithms. Appl Opt **50**, C239–C245 (2011)
9. Kim, S.W., Kim, G.H.: Thickness-profile measurement of transparent thin-film layers by white-light scanning interferometry. Appl Opt **38**, 5968–6973 (1999)
10. Choi, S., Otsuki, K., Sasaki, O., Suzuki, T.: Profile measurement of glass sheet using multiple wavelength backpropagation interferometry. Appl Opt **52**, 3726–3731 (2013)